# Ultrafast characterization of plasma critical surface evolution in inertial confinement fusion experiments with chirped laser pulses

**Linjun Li,[1,2, a)] Zhantao Lu,[1,2, a)] Xinglong Xie,[1,2, b)] Meizhi Sun,[1, a)] Xiao Liang,[1] Qingwei Yang,[1] Ailin Guo,[1] Ping Zhu,[1] Xuejie Zhang,[1] Dongjun Zhang,[1] Hao Xue,[1,2] Guoli Zhang,[1,2] Rashid Ul Haq,[1,2] Haidong Zhu,[1] Jun Kang,[1] Jianqiang Zhu[1,2, b)]**

[1] *National Laboratory on High Power Laser and Physics, Shanghai Institute of Optics and Fine Mechanics, Chinese Academy of Sciences, Shanghai 201800, People's Republic of China*

[2] *Center of Materials Science and Optoelectronics Engineering, University of Chinese Academy of Sciences, No. 19(A), Yuquan Road, Shijingshan, Beijing 100049, People's Republic of China*

[a)] **Authors are contributed equal**
[b)] **Authors to whom correspondence should be addressed:** xiexl329@siom.ac.cn and jqzhu@siom.ac.cn

**Abstract** Laser-driven inertial confinement fusion (ICF) diagnostics play a crucial role in understanding the complex physical processes governing ICF and enabling ignition. During the ICF process, the interaction between the high-power laser and ablation material leads to the formation of a plasma critical surface, which reflects a significant portion of the driving laser, reducing the efficiency of laser energy conversion into implosive kinetic energy. Effective diagnostic methods for the critical surface remain elusive. In this work, we propose a novel optical diagnostic approach to investigate the plasma critical surface.



10.1017/hpl.2025.4

This method has been experimentally validated, providing new insights into the critical surface morphology and dynamics. This advancement represents a significant step forward in ICF diagnostic capabilities, with the potential to inform strategies for enhancing the uniformity of the driving laser and target surface, ultimately improving the efficiency of converting laser energy into implosion kinetic energy and enabling ignition.

*Key words: inertial confinement fusion (ICF), laser-plasma interaction, critical surface evolution, plasma diagnostic techniques, direct drive*

## I. INTRODUCTION

The exploration of controlled fusion energy has been ongoing for more than half a century [1]. Laser inertial confinement fusion (ICF) is one of the most promising paths to achieve thermonuclear ignition, and has achieved the tremendous advancements in both scientific understanding and engineering aspects [2]. The first laboratory achievement of target gain $G_{target} > 1$ was reported at the US National Ignition Facility (NIF) in December 2022 [3], demonstrating the potential of the laboratory fusion. Both direct and indirect drives typically employ spherical targets. As the target surface absorbs laser energy and undergoes ablation, the pressure causes the remaining ablation layer and the DT fuel shell to implode inward. When the implosion reaches its minimum radius, a hot spot of DT forms, surrounded by colder, denser DT fuel [4]. Low-mode asymmetries are the dominant factor that degrades implosion performance. In addition, mixing of the ablation layer and the fuel also causes significant fuel preheating, further degrading implosion performance [2]. Improving the coupling of laser energy into target kinetic energy is a key to achieve the ignition. Laser-plasma instabilities [5], such that arise from the



https://doi.org/10.1017/hpl.2025.4 Published online by Cambridge University Press

interaction between the driving laser and the ablation plasma, can limit the absorption of laser energy and also accelerate electrons to the DT fuel layer, thereby reducing the final compression and preventing the ignition process [6]. Precise shaping and control of the driving laser pulse is a key step in the Inertial Confinement Fusion (ICF) process to reduce Rayleigh-Taylor (RT) instabilities and improve energy coupling efficiency [7]. When the laser interacts with the ablation layer, a critical surface is formed, and most of the laser energy is absorbed by the coronal region due to reflection at this critical surface, limiting the effective conversion to implosion kinetic energy [1,2,4-7]. We believe that understanding the evolution of the critical surface during the laser-ablation layer interaction will play an important role in improving the conversion efficiency of laser energy to fuel kinetic energy. Therefore, exploring the temporal evolution of the critical surface can provide a guidance for controlling the driving laser, adjusting the laser pulse pointing, and designing of the target, laying the foundation for ultimately achieving ignition.

To explore the complex physical processes in Inertial Confinement Fusion (ICF) and improve the coupling of laser energy to the target, various diagnostic techniques have been developed, such as VISAR [8], X-ray imaging [9], and X-ray spectroscopy [10]. VISAR measures the velocity of moving surfaces by recording the Doppler shift of the reflected light. VISAR is a critical diagnostic tool in ICF and high-energy density research, as it can be used to measure the velocity of rapidly moving surfaces (typically ~0.1 km/s to >100 km/s) [11-15], measure equations of state [16], characterize the strength and structure of materials under extreme conditions [17], and optimize the temporal pulse shape of the implosion laser in ICF experiments [18]. X-ray imaging can record the information about the shape, volume, and temperature of the plasma, providing valuable feedback for adjusting experimental parameters. Pinhole imaging is



https://doi.org/10.1017/hpl.2025.4 Published online by Cambridge University Press

the most commonly used X-ray imaging diagnostic, as pinholes are easy to fabricate, position and be easily replaced if damaged [19]. The principle of pinhole X-ray imaging is similar to that of visible light pinhole imaging, and the spatial resolution is limited by geometric optics and diffraction. X-ray spectroscopy can be used to diagnose the mixing of ablator material into the hot spot in indirect-drive experiments [20] and to characterize the state of the target [21].

Many of the aforementioned diagnostic techniques often work with streak cameras and rely on algorithmic reconstruction to obtain plasma parameters. Furthermore, existing diagnostic methods tend to focus on the compressed core region, lacking diagnostics for the critical surface of the ablation plasma. We believe that the lack of understanding of the evolution of the plasma critical surface hinders the improvement of laser energy coupling efficiency. In this paper, we propose an all-optical diagnostic method based on ultrashort lasers to diagnose the critical surface formed by the interaction between the driving laser and the ablation layer in the ICF process, and experimentally verify the feasibility of the method.

## II. METHODS

We have developed a femtosecond laser-based fusion plasma measurement method. This method utilizes the rich frequency components of femtosecond lasers, using dispersion to temporally stretch the probe pulse, thus make the probe with time-frequency chirp, as shown in the figure below. We use a pulse with a center wavelength of 808 nm and a pulse width of 30 fs, which is then stretched to 1.7 ns by a pulse stretcher, with a spectral range of 780-860 nm. It is a flat-top s-polarized pulse with a fast rise of approximately 100ps. This probe beam is then made to interact with the evolving plasma under study, where different wavelengths can record information at different instant time. Finally, we record the spectral changes of the probe beam before and after the measurements, and by analyzing these changes, we can obtain the expansion



https://doi.org/10.1017/hpl.2025.4 Published online by Cambridge University Press

velocity of the critical surface as well as the time-resolved evolution of the critical surface morphology.

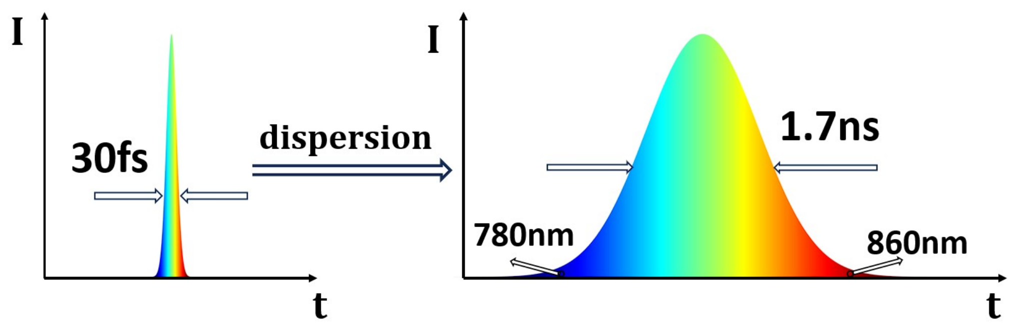


**Figure 1.** A femtosecond laser pulse with a center wavelength of 808 nm and a pulse duration of 30 fs is coupled into a pulse stretcher. The pulse stretcher introduces group velocity dispersion, which stretches temporally the pulse duration by frequency-time chirp. This results in the generation of a chirped probe pulse with a duration of 1.7 ns and a spectral range of 780 nm to 860 nm. The time-dependent wavelength distribution of this stretched probe pulse allows for time-resolved probing of the evolving plasma dynamics under investigation.

In a linearly temporal stretched femtosecond laser pulse, different time points correspond to different wavelengths. When this chirped probe pulse interacts with the critical surface, the spectral components of the measured probe pulse are recorded using a spectrometer. By analyzing and comparing the spectral changes of the probe pulse before and after the interaction with the critical surface, the evolution dynamics of the critical surface within the probe pulse duration can be obtained. To evaluate the velocity of the critical surface, the probe beam is first compressed to a narrow pulse of several tens of femtoseconds using a parallel grating compressor, and the pulse width is measured using an autocorrelator before the probe beam interacts with the plasma critical surface. After the probe beam interacts with the plasma, it is



https://doi.org/10.1017/hpl.2025.4 Published online by Cambridge University Press

compressed again using the same parallel grating compressor, and the change in the probe beam pulse width Δt can be measured. This change in pulse width Δt reflects the expansion velocity v of the plasma critical surface. By analysis, a relationship can be established between the change in pulse width Δt, the probe beam pulse width τ, the incidence angle θ, and the critical surface expansion velocity v, as shown in the following equation,

$$\Delta t = \frac{2v\tau}{\cos\theta \times c} \tag{1}$$

where c is the speed of light. The CCD image recorded captures the temporal evolution of the critical surface topography. The spatial information on the CCD corresponds to the temporal evolution of the critical surface, with each position on the CCD representing a different time delay relative to the initial probe pulse.

## III. EXPERIMENT SETUP

The experiment is conducted with SGII nanosecond laser facility and SG-5PW femtosecond laser system. The probe beam employed in our experiment is sourced from the SG-5PW front - end and expanded to about 100mm×100mm in size [22-24], in which two optical parametric chirped pulse amplification (OPCPA) links make up the whole beam, and each of the OPCPA link has two BBO crystals. These BBO crystals are cutting in TYPE 1 configuration, with a phase matching angle of 23.8° and a non-collinear angle of 2.36° within the crystal. The frequency-doubled Nd: YAG laser independently developed by our laboratory is used as the pump source of the OPCPA links at a repetition rate of 1Hz. The femtosecond seed pulse is generated by a commercial Ti: Sapphire laser (FEMTO LASERS). The seed pulse width is 10fs, the repetition rate 75MHz, and the average power 150mW. After passing through the stretcher,



https://doi.org/10.1017/hpl.2025.4 Published online by Cambridge University Press

the seed pulse is temporally broadened into a chirped pulse with a full width at half maximum (FWHM) of 0.85ns and a chirp rate of 21.3ps/nm.

The experimental setup utilizes one beam of the SGII, a 526 nm, 1 ns, 200 J laser pulse as the driving laser. It drives the formation of fusion plasma from a CD target (a commonly used low-Z ablator material in ICF experiments). The focused peak power density is $1\times10^{15}$ W/cm$^2$. The temporal profile of the drive laser is a square wave, with a rise time of approximately 110 ps. The probe beam is a chirped pulse, as mentioned in the previous section. As shown in Figure 2, this time-resolved imaging technique leverages the interaction between the probe beam and the plasma critical surface. The driving beam is incident vertically on the target surface, while the probe beam is focused by an off-axis parabolic mirror and incident on the target surface at an angle of 21°. In the experiment, the time synchronization between the drive laser and the probe beam was measured at the target location using a photodetector. The photodetector's response time is 60 ps, and the accuracy of the time synchronization is 10 ps RMS. The time delay mentioned in the subsequent text refers to the temporal difference between the leading edges of the two laser pulses.

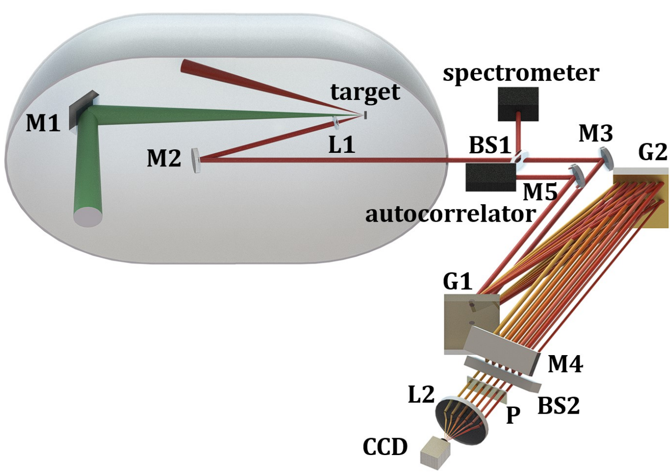


**Figure 2.** The experimental setup consists of the following optical components: M1-M7 are reflective mirrors, BS1 and BS2 are beam splitters, L1 and L2 are focusing lenses, G1 and G2 are gold-coated diffraction



https://doi.org/10.1017/hpl.2025.4 Published online by Cambridge University Press

gratings, and P is an aperture plate. Notably, M1, M2, and the target are all situated within a vacuum target chamber.

After interacting with the fusion plasma, the probe beam is collimated by lens L1 and reflected by mirror M2 to be extracted from the vacuum target chamber. The probe beam is then split by beam splitter BS1, with one portion directed to a spectrometer to measure the probe spectrum. The other reflected by M3 is sent through a pair of diffraction gratings G1 and G2 to recompress the probe beam back to its original femtosecond pulse duration, which is then reflected by mirror M4 and directed into an autocorrelator to measure the pulse width of the compressed probe beam. The remaining portion of the probe beam is diffracted by the grating pair G1 and G2, collimated, and transmitted through BS2. This beam then passes through an aperture plate P (with six pinholes corresponding to wavelengths of 809 nm, 815 nm, 821 nm, 826 nm, 833 nm, and 837 nm) and lens L2, and is imaged onto a CCD camera. By comparing the brightness of the spots on the CCD before and after the injection of the drive beam, the synchronization between the drive and probe beams can be assessed, providing a reference for adjusting the time delay between the two beams.

## IV. RESULTS AND DISCUSSION

In order to further analyze the experimental data, we utilized the radiation magnetohydrodynamics code FLASH [25-26] to perform simulations. FLASH is capable of multi-temperature treatment of the plasma, enabling it to model high energy density physics experiments driven by lasers. Based on the laser and target parameters in the experiment, we conducted laser-driven ablation simulations on a 50 μm thick, 1 g/cm$^3$ density CD target using a 526 nm wavelength, $1\times10^{15}$ W/cm$^2$ intensity, 1 ns duration laser. The initial setup of the



https://doi.org/10.1017/hpl.2025.4 Published online by Cambridge University Press

simulation is shown in Figure 3. The simulation domain size was 280 μm × 80 μm with a grid size of 0.1 μm. Subsequently, we reconstructed the experimental optical path of the probe beam.

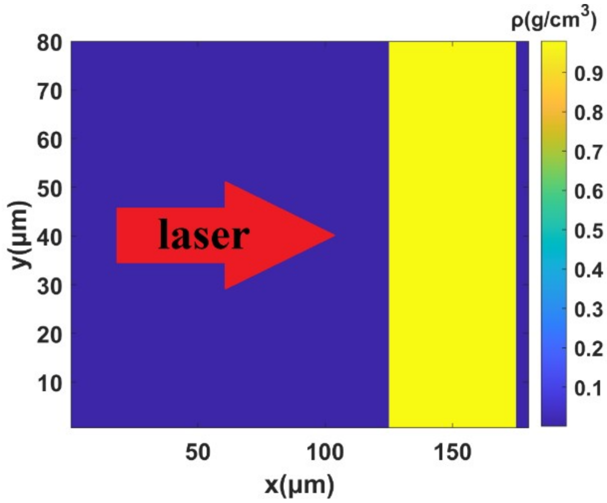


**Figure 3.** The initial conditions for the simulation

At time t, the probe beam wavelength components λ were incident on the laser-ablated plasma at uniform angles θ ranging from 16° to 26°. The different wavelengths λ and incident angles θ correspond to different densities of the reflection surface. Based on the FLASH simulation results, we obtained the critical surface position, velocity, reflectivity, and tangential angle (reflecting the critical surface morphology) at that time and location. We then calculated the Doppler shift in wavelength and the reflection angle due to the Doppler effect, and performed ray tracing to determine the portion of the light that could pass through the subsequent optical components and reach the spectrometer, thereby obtaining the simulated spectrometer signal. The results calculated without considering the changes in surface morphology at the critical surface are shown in Figures 4(a), 4(c), and 4(e), where the red line represents the spectrum received by the spectrometer in the experiment, and the blue line shows the calculated spectrum. Without considering the changes in surface morphology, the wavelength range that can reach the spectrometer is very wide, and the periodic peaks and valleys reflect the oscillation of the critical



https://doi.org/10.1017/hpl.2025.4 Published online by Cambridge University Press

surface driven by the hydrodynamic force. When the changes in surface morphology are considered, the calculated results are shown in Figures 4(b), 4(d), and 4(f), where the red line represents the spectrum received by the spectrometer in the experiment, and the blue line shows the calculated spectrum. The calculated results agree well with the experimental results.

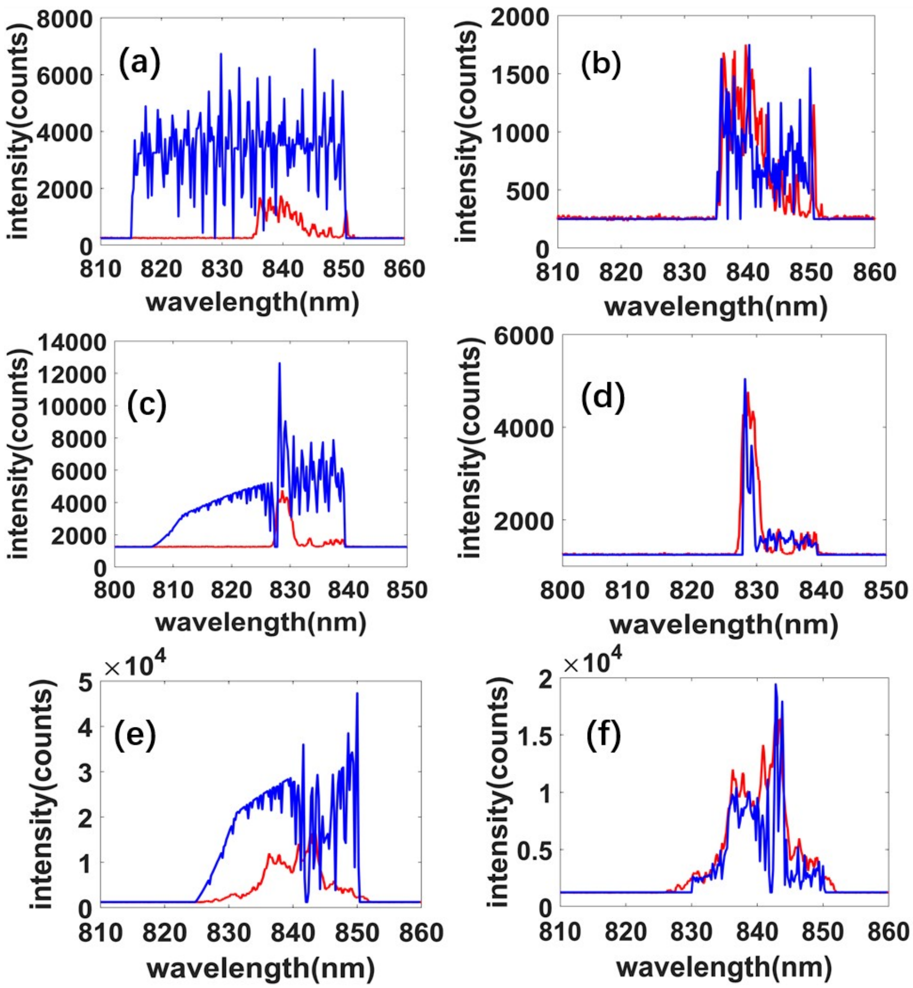


**Figure 4.** Measured probe beam spectrum (red line) and calculated spectrum (blue line). Without considering the change in the critical surface morphology, the probe beam is delayed relative to the drive beam by (a) 250 ps, (c) 940 ps, and (e) 1035 ps. Considering the change in the critical surface morphology, the probe beam is delayed relative to the drive beam by(b) 250 ps, (d) 940 ps, and (f) 1035 ps.



https://doi.org/10.1017/hpl.2025.4 Published online by Cambridge University Press

To explain the changes in the spectrum, we consider the critical surface in the probe beam interaction region as a curved arc. In the initial phase of the interaction of the probe with the plasma surface, most of the probe is reflected by the surface which works like a convex mirror, so only a small part light energy enters into the subsequent optical path. After some time, the curvature of the curved arc decreases due to the probe beam's action, and the portion entering the subsequent optical path is maximized. Meanwhile, the reflective mirror formed by the two ends of the curved arc rotates towards the direction perpendicular to the probe beam due to the probe beam's action. After several hundred picoseconds, the reflected probe beam can no longer enter the subsequent optical path due to the change in the reflection angle. The changes in the surface morphology of the critical surface are caused by the actual surface profile of the planar target used in the experiment and the non-uniformity of the driving laser. Therefore, our measurement method can reflect the time-dependent changes in the surface morphology of the critical surface. Additionally, it is worth noting that the different spectra at different delays are due to the changes in the position of the critical surface, and the cessation of the driving laser results in the termination of the isothermal expansion, leading to changes in the density distribution of the plasma induced by the rarefaction wave.

The CCD images before and after the drive beam injection are shown in Figure 5.



https://doi.org/10.1017/hpl.2025.4 Published online by Cambridge University Press

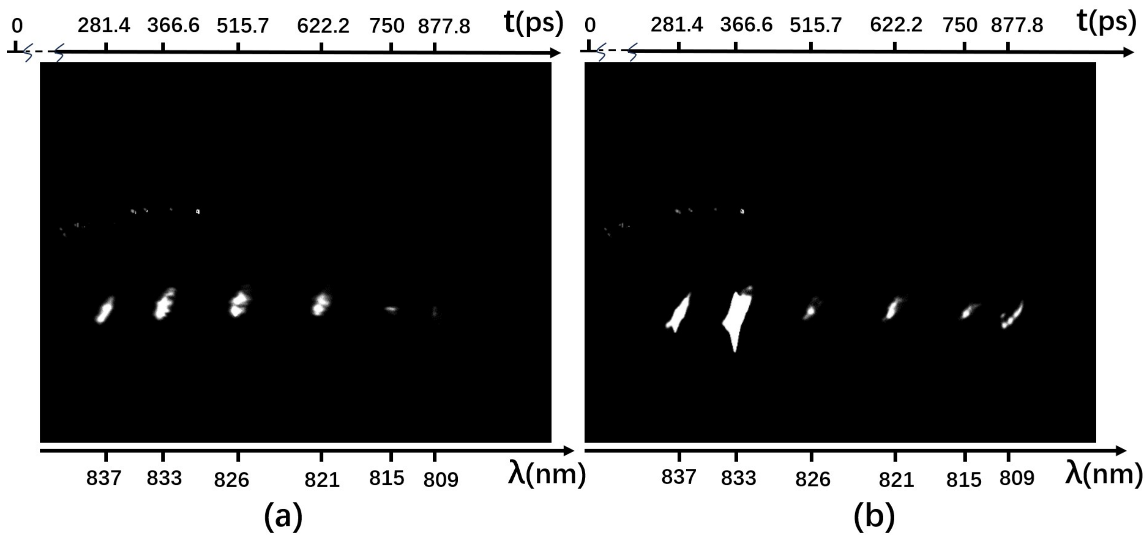


**Figure 5.** the image on the CCD sensor (a) without driving laser (b) with driving laser. Specifically, the zero-point in the figure represents the moment when the probe beam begins to interact with the target.

In the absence of the drive beam injection, the light spot on the CCD corresponds to the reflection of the probe beam from the target surface itself, exhibiting relatively weak brightness. Starting from the image of the 5th hole (corresponding to a wavelength of 815 nm), i.e., approximately 750 ps after the probe beam interaction, the brightness of the light spot is significantly reduced due to the damage of the target under laser irradiation. After the drive beam injection, the light spot on the CCD is attributed to the reflection of the probe beam from the plasma critical surface, with a relatively high reflectivity exceeding 70%, resulting in an enhanced brightness of the light spot. Interestingly, we observed that the light spots in the first two holes are larger, while the light spot in the third hole is considerably smaller. Based on the simulation results, this phenomenon can be attributed to the presence of the pre-pulse. The pre-pulse arrives before the probe beam and forms an initial plasma distribution. The probe beam, having a longer wavelength and a lower critical density, corresponds to a relatively flat critical surface morphology. Additionally, the low-density region is farther away from the target surface,



https://doi.org/10.1017/hpl.2025.4 Published online by Cambridge University Press

and the change in object distance leads to a larger image on the CCD. In this case, the light spot on the CCD represents the reflection image of the plasma critical surface within the probe beam range. The main pulse arrives between the time corresponding to the second hole and the third hole. Due to the high light intensity, the plasma within the main pulse light spot is rapidly compressed towards the target surface, while the surrounding plasma is also affected, forming a "funnel" shape. In this scenario, the light spot on the CCD corresponds to the reflection image of the plasma critical surface within the main pulse light spot, and the other parts within the probe beam range cannot enter the CCD due to the change in the plasma critical surface morphology.

Based on the measurements from the autocorrelation setup, we have calculated the expansion velocity of the critical surface, as shown in Figure 6. Figure 6(a) presents the autocorrelation signals obtained at different delays between the probe beam and the main pulse leading edge, where the delay refers to the relative time between the main pulse leading edge and the probe beam leading edge. To avoid the gradual change in the critical surface morphology under the influence of the probe beam, as discussed previously, we have extracted the 836-850nm portion of the probe beam, corresponding to a broadened pulse width of 300 ps.

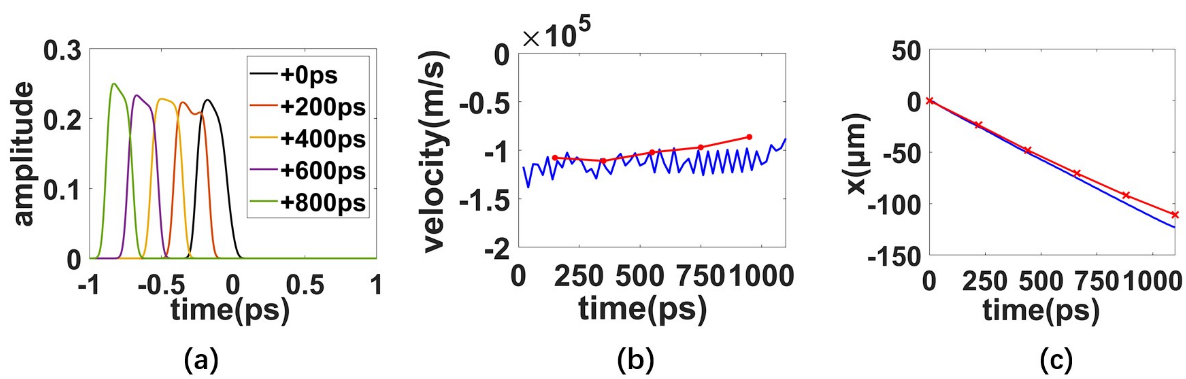


**Figure 6.** (a) Autocorrelation signals at different time delays (0 ps, 200 ps, 400 ps, 600 ps, 800 ps). (b) Critical surface expansion velocity measured from the autocorrelation signals (red line) and obtained from numerical simulations (blue line). (c) Critical surface position as a function of time measured from the



https://doi.org/10.1017/hpl.2025.4 Published online by Cambridge University Press

autocorrelation signals (red line) and obtained from numerical simulations (blue line). (The negative sign in Figures 6(b) and 6(c) indicates that the direction of the plasma critical surface movement is opposite to the direction of the drive laser)

Using Eq. (1), we can calculate the critical surface expansion velocity at different time points and compare it with the results from numerical simulations, as shown in Figure 6(b). The oscillation in the simulated velocity is due to the effect of radiation pressure, which causes the critical surface to oscillate. In contrast, the autocorrelation signal-based velocity represents the average motion of the critical surface within the 300 ps interaction with the probe beam. Furthermore, we have also calculated the critical surface position at different time points based on the measured velocity and compared it with the numerical simulation results, as shown in Figure 6(c). The measured results agree well with the numerical simulation, and the critical surface expansion velocity is in the range of $1\times10^5$-$2\times10^5$ m/s, consistent with the previous reports [22]. The deviations in the results can be attributed to two factors: first, the measurement error of the autocorrelation setup, and second, the fact that for the 836-850 nm probe beam, the shorter wavelength part corresponds to a higher critical density and reflects at a position closer to the target, resulting in a smaller change in the optical path compared to the case where the wavelength is constant, leading to an underestimation of the critical surface expansion velocity.

## V. CONCLUSIONS

We have developed a novel optical measurement technique capable of probing the surface deformation and expansion velocity of the critical surface within the ablation layer during the inertial confinement fusion (ICF) process. This innovative approach provides new insights into the underlying physical phenomena governing ICF, which can inform strategies to enhance the uniformity of the drive laser and target surface. Ultimately, this advancement has the potential to improve the efficiency of converting laser energy into implosion kinetic energy.

Correspondence to: NO.390 Qinghe Road, JiaDing District, Shanghai. Email: xiexl329@siom.ac.cn and jqzhu@siom.ac.cn

## Acknowledgement

This work is supported by the National Natural Science Foundation of China (NSFC) (12074399, 12204500, 12004403), Key projects of intergovernmental international scientific and technological innovation cooperation (2021YFE0116700), Shanghai Natural Science Foundation (20ZR1464400), and Shanghai Sailing Program (22YF1455300)

## References

1. O. A. Hurricane, P. K. Patel, R. Betti, D. H. Froula, S. P. Regan, S. A. Slutz, M. R. Gomez, and M. A. Sweeney, "Physics principles of inertial confinement fusion and U.S. program overview," Rev. Mod. Phys. 95, 025005 (2023). DOI: https://doi.org/10.1103/RevModPhys.95.025005
2. R. S. Craxton, K. S. Anderson, T. R. Boehly, V. N. Goncharov, D. R. Harding, J. P. Knauer, R. L. McCrory, P. W. McKenty, D. D. Meyerhofer, J. F. Myatt, A. J. Schmitt, J. D. Sethian, R. W. Short, S. Skupsky, W. Theobald, W. L. Kruer, K. Tanaka, R. Betti, T. J. B. Collins, J. A. Delettrez, S. X. Hu, J. A. Marozas, A. V. Maximov, D. T. Michel, P. B. Radha, S. P. Regan, T. C. Sangster, W. Seka, A. A. Solodov, J. M. Soures, C. Stoeckl, and J. D. Zuegel, "Direct-drive inertial confinement fusion: A review," Phys. Plasmas 22(2015). DOI: https://doi.org/10.1063/1.4934714
3. H. Abu-Shawareb and R. Acree and P. Adams and J. Adams and B. Addis and R. Aden and P. Adrian and B. B. Afeyan and M. Aggleton and L. Aghaian and A. Aguirre and D. Aikens and J. Akre and F. Albert and M. Albrecht and B. J. Albright and J. Albritton and J. Alcala and C. Alday and D. A. Alessi and N. Alexander and J. Alfonso and N. Alfonso and E. Alger and S. J. Ali and Z. A. Ali and A. Allen and W. E. Alley and P. Amala and P. A. Amendt and P. Amick and S. Ammula and C. Amorin and D. J. Ampleford and R. W. Anderson and T. Anklam and N. Antipa and B. Appelbe and C. Aracne-Ruddle and E. Araya and T. N. Archuleta and M. Arend and P. Arnold and T. Arnold and A. Arsenlis



https://doi.org/10.1017/hpl.2025.4 Published online by Cambridge University Press

and J. Asay and L. J. Atherton and D. Atkinson and R. Atkinson and J. M. Auerbach and B. Austin and L. Auyang and A. A. S. Awwal and N. Aybar and J. Ayers and S. Ayers and T. Ayers and S. Azevedo and B. Bachmann and C. A. Back and J. Bae and D. S. Bailey and J. Bailey and T. Baisden and K. L. Baker and H. Baldis and D. Barber and M. Barberis and D. Barker and A. Barnes and C. W. Barnes and M. A. Barrios and C. Barty and I. Bass and S. H. Batha and S. H. Baxamusa and G. Bazan and J. K. Beagle and R. Beale and B. R. Beck and J. B. Beck and M. Bedzyk and R. G. Beeler and R. G. Beeler and W. Behrendt and L. Belk and P. Bell and M. Belyaev and J. F. Benage and G. Bennett and L. R. Benedetti and L. X. Benedict and R. L. Berger and T. Bernat and L. A. Bernstein and B. Berry and L. Bertolini and G. Besenbruch and J. Betcher and R. Bettenhausen and R. Betti and B. Bezzerides and S. D. Bhandarkar and R. Bickel and J. Biener and T. Biesiada and K. Bigelow and J. Bigelow-Granillo and V. Bigman and R. M. Bionta and N. W. Birge and M. Bitter and A. C. Black and R. Bleile and D. L. Bleuel and E. Bliss and E. Bliss and B. Blue and T. Boehly and K. Boehm and C. D. Boley and R. Bonanno and E. J. Bond and T. Bond and M. J. Bonino and M. Borden and J. L. Bourgade and J. Bousquet and J. Bowers and M. Bowers and R. Boyd and D. Boyle and A. Bozek and D. K. Bradley and K. S. Bradley and P. A. Bradley and L. Bradley and L. Brannon and P. S. Brantley and D. Braun and T. Braun and K. Brienza-Larsen and R. Briggs and T. M. Briggs and J. Britten and E. D. Brooks and D. Browning and M. W. Bruhn and T. A. Brunner and H. Bruns and G. Brunton and B. Bryant and T. Buczek and J. Bude and L. Buitano and S. Burkhart and J. Burmark and A. Burnham and R. Burr and L. E. Busby and B. Butlin and R. Cabeltis and M. Cable and W. H. Cabot and B. Cagadas and J. Caggiano and R. Cahayag and S. E. Caldwell and S. Calkins and D. A. Callahan and J. Calleja-Aguirre and L. Camara and D. Camp and E. M. Campbell and J. H. Campbell and B. Carey and R. Carey and K. Carlisle and L. Carlson and L. Carman and J. Carmichael and A. Carpenter and C. Carr and J. A. Carrera and D. Casavant and A. Casey and D. T. Casey and A. Castillo and E. Castillo and J. I. Castor and C. Castro and W. Caughey and R. Cavitt and J. Celeste and P. M. Celliers and C. Cerjan and G. Chandler and B. Chang and C. Chang and J. Chang and L. Chang and R. Chapman and T. D. Chapman and L. Chase and H. Chen and H. Chen and K. Chen and L. Y. Chen and B. Cheng and J. Chittenden and C. Choate and J. Chou and R. E. Chrien and M. Chrisp and K. Christensen and M. Christensen and N. S. Christiansen and A. R. Christopherson and M. Chung and J. A. Church and A. Clark and D. S. Clark and K. Clark and R. Clark and L. Claus and B. Cline and J. A. Cline and J. A. Cobble and K. Cochrane and B. Cohen and S. Cohen and M. R. Collette and G. W. Collins and L. A. Collins and T. J. B. Collins and A. Conder and B. Conrad and M. Conyers and A. W. Cook and D. Cook and R. Cook and J. C. Cooley and G. Cooper and T. Cope and S. R. Copeland and F. Coppari and J. Cortez and J. Cox and D. H. Crandall and J. Crane and R. S. Craxton and M. Cray and A. Crilly and J. W. Crippen and D. Cross and M. Cuneo and G. Cuotts and C. E. Czajka and D. Czechowicz and T. Daly and P. Danforth and C. Danly and R. Darbee and B. Darlington and P. Datte and L. Dauffy and G. Davalos and S. Davidovits and P. Davis and J. Davis and S. Dawson and R. D. Day and T. H. Day and M. Dayton and C. Deck and C. Decker and C. Deeney and K. A. DeFriend and G. Deis and N. D. Delamater and J. A. Delettrez and R. Demaret and S. Demos and S. M. Dempsey and R. Desjardin and T. Desjardins and M. P. Desjarlais and E. L. Dewald and J. DeYoreo and S. Diaz and G. Dimonte and T. R. Dittrich and L. Divol and S. N. Dixit and J. Dixon and A. Do and E.



https://doi.org/10.1017/hpl.2025.4 Published online by Cambridge University Press

S. Dodd and D. Dolan and A. Donovan and M. Donovan and T. Döppner and C. Dorrer and N. Dorsano and M. R. Douglas and D. Dow and J. Downie and E. Downing and M. Dozieres and V. Draggoo and D. Drake and R. P. Drake and T. Drake and G. Dreifuerst and O. Drury and D. F. DuBois and P. F. DuBois and G. Dunham and M. Durocher and R. Dylla-Spears and A. K. L. Dymoke-Bradshaw and B. Dzenitis and C. Ebbers and M. Eckart and S. Eddinger and D. Eder and D. Edgell and M. J. Edwards and P. Efthimion and J. H. Eggert and B. Ehrlich and P. Ehrmann and S. Elhadj and C. Ellerbee and N. S. Elliott and C. L. Ellison and F. Elsner and M. Emerich and K. Engelhorn and T. England and E. English and P. Epperson and R. Epstein and G. Erbert and M. A. Erickson and D. J. Erskine and A. Erlandson and R. J. Espinosa and C. Estes and K. G. Estabrook and S. Evans and A. Fabyan and J. Fair and R. Fallejo and N. Farmer and W. A. Farmer and M. Farrell and V. E. Fatherley and M. Fedorov and E. Feigenbaum and T. Fehrenbach and M. Feit and B. Felker and W. Ferguson and J. C. Fernandez and A. Fernandez-Panella and S. Fess and J. E. Field and C. V. Filip and J. R. Fincke and T. Finn and S. M. Finnegan and R. G. Finucane and M. Fischer and A. Fisher and J. Fisher and B. Fishler and D. Fittinghoff and P. Fitzsimmons and M. Flegel and K. A. Flippo and J. Florio and J. Folta and P. Folta and L. R. Foreman and C. Forrest and A. Forsman and J. Fooks and M. Foord and R. Fortner and K. Fournier and D. E. Fratanduono and N. Frazier and T. Frazier and C. Frederick and M. S. Freeman and J. Frenje and D. Frey and G. Frieders and S. Friedrich and D. H. Froula and J. Fry and T. Fuller and J. Gaffney and S. Gales and B. Le Galloudec and K. K. Le Galloudec and A. Gambhir and L. Gao and W. J. Garbett and A. Garcia and C. Gates and E. Gaut and P. Gauthier and Z. Gavin and J. Gaylord and C. G. R. Geddes and M. Geissel and F. Génin and J. Georgeson and H. Geppert-Kleinrath and V. Geppert-Kleinrath and N. Gharibyan and J. Gibson and C. Gibson and E. Giraldez and V. Glebov and S. G. Glendinning and S. Glenn and S. H. Glenzer and S. Goade and P. L. Gobby and S. R. Goldman and B. Golick and M. Gomez and V. Goncharov and D. Goodin and P. Grabowski and E. Grafil and P. Graham and J. Grandy and E. Grasz and F. R. Graziani and G. Greenman and J. A. Greenough and A. Greenwood and G. Gregori and T. Green and J. R. Griego and G. P. Grim and J. Grondalski and S. Gross and J. Guckian and N. Guler and B. Gunney and G. Guss and S. Haan and J. Hackbarth and L. Hackel and R. Hackel and C. Haefner and C. Hagmann and K. D. Hahn and S. Hahn and B. J. Haid and B. M. Haines and B. M. Hall and C. Hall and G. N. Hall and M. Hamamoto and S. Hamel and C. E. Hamilton and B. A. Hammel and J. H. Hammer and G. Hampton and A. Hamza and A. Handler and S. Hansen and D. Hanson and R. Haque and D. Harding and E. Harding and J. D. Hares and D. B. Harris and J. A. Harte and E. P. Hartouni and R. Hatarik and S. Hatchett and A. A. Hauer and M. Havre and R. Hawley and J. Hayes and J. Hayes and S. Hayes and A. Hayes-Sterbenz and C. A. Haynam and D. A. Haynes and D. Headley and A. Heal and J. E. Heebner and S. Heerey and G. M. Heestand and R. Heeter and N. Hein and C. Heinbockel and C. Hendricks and M. Henesian and J. Heninger and J. Henrikson and E. A. Henry and E. B. Herbold and M. R. Hermann and G. Hermes and J. E. Hernandez and V. J. Hernandez and M. C. Herrmann and H. W. Herrmann and O. D. Herrera and D. Hewett and R. Hibbard and D. G. Hicks and D. P. Higginson and D. Hill and K. Hill and T. Hilsabeck and D. E. Hinkel and D. D. Ho and V. K. Ho and J. K. Hoffer and N. M. Hoffman and M. Hohenberger and M. Hohensee and W. Hoke and D. Holdener and F. Holdener and J. P. Holder and B. Holko and D. Holunga and J. F. Holzrichter and J. Honig and D. Hoover



https://doi.org/10.1017/hpl.2025.4 Published online by Cambridge University Press

and D. Hopkins and L. F. Berzak Hopkins and M. Hoppe and M. L. Hoppe and J. Horner and R. Hornung and C. J. Horsfield and J. Horvath and D. Hotaling and R. House and L. Howell and W. W. Hsing and S. X. Hu and H. Huang and J. Huckins and H. Hui and K. D. Humbird and J. Hund and J. Hunt and O. A. Hurricane and M. Hutton and K. H. K. Huynh and L. Inandan and C. Iglesias and I. V. Igumenshchev and I. Ivanovich and N. Izumi and M. Jackson and J. Jackson and S. D. Jacobs and G. James and K. Jancaitis and J. Jarboe and L. C. Jarrott and D. Jasion and J. Jaquez and J. Jeet and A. E. Jenei and J. Jensen and J. Jimenez and R. Jimenez and D. Jobe and Z. Johal and H. M. Johns and D. Johnson and M. A. Johnson and M. Gatu Johnson and R. J. Johnson and S. Johnson and S. A. Johnson and T. Johnson and K. Jones and O. Jones and M. Jones and R. Jorge and H. J. Jorgenson and M. Julian and B. I. Jun and R. Jungquist and J. Kaae and N. Kabadi and D. Kaczala and D. Kalantar and K. Kangas and V. V. Karasiev and M. Karasik and V. Karpenko and A. Kasarky and K. Kasper and R. Kauffman and M. I. Kaufman and C. Keane and L. Keaty and L. Kegelmeyer and P. A. Keiter and P. A. Kellett and J. Kellogg and J. H. Kelly and S. Kemic and A. J. Kemp and G. E. Kemp and G. D. Kerbel and D. Kershaw and S. M. Kerr and T. J. Kessler and M. H. Key and S. F. Khan and H. Khater and C. Kiikka and J. Kilkenny and Y. Kim and Y. J. Kim and J. Kimko and M. Kimmel and J. M. Kindel and J. King and R. K. Kirkwood and L. Klaus and D. Klem and J. L. Kline and J. Klingmann and G. Kluth and P. Knapp and J. Knauer and J. Knipping and M. Knudson and D. Kobs and J. Koch and T. Kohut and C. Kong and J. M. Koning and P. Koning and S. Konior and H. Kornblum and L. B. Kot and B. Kozioziemski and M. Kozlowski and P. M. Kozlowski and J. Krammen and N. S. Krasheninnikova and C. M. Krauland and B. Kraus and W. Krauser and J. D. Kress and A. L. Kritcher and E. Krieger and J. J. Kroll and W. L. Kruer and M. K. G. Kruse and S. Kucheyev and M. Kumbera and S. Kumpan and J. Kunimune and E. Kur and B. Kustowski and T. J. T. Kwan and G. A. Kyrala and S. Laffite and M. Lafon and K. LaFortune and L. Lagin and B. Lahmann and B. Lairson and O. L. Landen and T. Land and M. Lane and D. Laney and A. B. Langdon and J. Langenbrunner and S. H. Langer and A. Langro and N. E. Lanier and T. E. Lanier and D. Larson and B. F. Lasinski and D. Lassle and D. LaTray and G. Lau and N. Lau and C. Laumann and A. Laurence and T. A. Laurence and J. Lawson and H. P. Le and R. R. Leach and L. Leal and A. Leatherland and K. LeChien and B. Lechleiter and A. Lee and M. Lee and T. Lee and R. J. Leeper and E. Lefebvre and J. P. Leidinger and B. LeMire and R. W. Lemke and N. C. Lemos and S. Le Pape and R. Lerche and S. Lerner and S. Letts and K. Levedahl and T. Lewis and C. K. Li and H. Li and J. Li and W. Liao and Z. M. Liao and D. Liedahl and J. Liebman and G. Lindford and E. L. Lindman and J. D. Lindl and H. Loey and R. A. London and F. Long and E. N. Loomis and F. E. Lopez and H. Lopez and E. Losbanos and S. Loucks and R. Lowe-Webb and E. Lundgren and A. P. Ludwigsen and R. Luo and J. Lusk and R. Lyons and T. Ma and Y. Macallop and M. J. MacDonald and B. J. MacGowan and J. M. Mack and A. J. Mackinnon and S. A. MacLaren and A. G. MacPhee and G. R. Magelssen and J. Magoon and R. M. Malone and T. Malsbury and R. Managan and R. Mancini and K. Manes and D. Maney and D. Manha and O. M. Mannion and A. M. Manuel and M. J. E. Manuel and E. Mapoles and G. Mara and T. Marcotte and E. Marin and M. M. Marinak and D. A. Mariscal and E. F. Mariscal and E. V. Marley and J. A. Marozas and R. Marquez and C. D. Marshall and F. J. Marshall and M. Marshall and S. Marshall and J. Marticorena and J. I. Martinez and D. Martinez and I. Maslennikov and D. Mason and R. J. Mason and L. Masse and W.

Massey and P. E. Masson-Laborde and N. D. Masters and D. Mathisen and E. Mathison and J. Matone and M. J. Matthews and C. Mattoon and T. R. Mattsson and K. Matzen and C. W. Mauche and M. Mauldin and T. McAbee and M. McBurney and T. McCarville and R. L. McCrory and A. M. McEvoy and C. McGuffey and M. McInnis and P. McKenty and M. S. McKinley and J. B. McLeod and A. McPherson and B. McQuillan and M. Meamber and K. D. Meaney and N. B. Meezan and R. Meissner and T. A. Mehlhorn and N. C. Mehta and J. Menapace and F. E. Merrill and B. T. Merritt and E. C. Merritt and D. D. Meyerhofer and S. Mezyk and R. J. Mich and P. A. Michel and D. Milam and C. Miller and D. Miller and D. S. Miller and E. Miller and E. K. Miller and J. Miller and M. Miller and P. E. Miller and T. Miller and W. Miller and V. Miller-Kamm and M. Millot and J. L. Milovich and P. Minner and J. L. Miquel and S. Mitchell and K. Molvig and R. C. Montesanti and D. S. Montgomery and M. Monticelli and A. Montoya and J. D. Moody and A. S. Moore and E. Moore and M. Moran and J. C. Moreno and K. Moreno and B. E. Morgan and T. Morrow and J. W. Morton and E. Moses and K. Moy and R. Muir and M. S. Murillo and J. E. Murray and J. R. Murray and D. H. Munro and T. J. Murphy and F. M. Munteanu and J. Nafziger and T. Nagayama and S. R. Nagel and R. Nast and R. A. Negres and A. Nelson and D. Nelson and J. Nelson and S. Nelson and S. Nemethy and P. Neumayer and K. Newman and M. Newton and H. Nguyen and J. M. G. Di Nicola and P. Di Nicola and C. Niemann and A. Nikroo and P. M. Nilson and A. Nobile and V. Noorai and R. C. Nora and M. Norton and M. Nostrand and V. Note and S. Novell and P. F. Nowak and A. Nunez and R. A. Nyholm and M. O'Brien and A. Oceguera and J. A. Oertel and A. L. Oesterle and J. Okui and B. Olejniczak and J. Oliveira and P. Olsen and B. Olson and K. Olson and R. E. Olson and Y. P. Opachich and N. Orsi and C. D. Orth and M. Owen and S. Padalino and E. Padilla and R. Paguio and S. Paguio and J. Paisner and S. Pajoom and A. Pak and S. Palaniyappan and K. Palma and T. Pannell and F. Papp and D. Paras and T. Parham and H. S. Park and A. Pasternak and S. Patankar and M. V. Patel and P. K. Patel and R. Patterson and S. Patterson and B. Paul and M. Paul and E. Pauli and O. T. Pearce and J. Pearcy and A. Pedretti and B. Pedrotti and A. Peer and L. J. Pelz and B. Penetrante and J. Penner and A. Perez and L. J. Perkins and E. Pernice and T. S. Perry and S. Person and D. Petersen and T. Petersen and D. L. Peterson and E. B. Peterson and J. E. Peterson and J. L. Peterson and K. Peterson and R. R. Peterson and R. D. Petrasso and F. Philippe and D. Phillion and T. J. Phipps and E. Piceno and L. Pickworth and Y. Ping and J. Pino and K. Piston and R. Plummer and G. D. Pollack and S. M. Pollaine and B. B. Pollock and D. Ponce and J. Ponce and J. Pontelandolfo and J. L. Porter and J. Post and O. Poujade and C. Powell and H. Powell and G. Power and M. Pozulp and M. Prantil and M. Prasad and S. Pratuch and S. Price and K. Primdahl and S. Prisbrey and R. Procassini and A. Pruyne and B. Pudliner and S. R. Qiu and K. Quan and M. Quinn and J. Quintenz and P. B. Radha and F. Rainer and J. E. Ralph and K. S. Raman and R. Raman and P. W. Rambo and S. Rana and A. Randewich and D. Rardin and M. Ratledge and N. Ravelo and F. Ravizza and M. Rayce and A. Raymond and B. Raymond and B. Reed and C. Reed and S. Regan and B. Reichelt and V. Reis and S. Reisdorf and V. Rekow and B. A. Remington and A. Rendon and W. Requieron and M. Rever and H. Reynolds and J. Reynolds and J. Rhodes and M. Rhodes and M. C. Richardson and B. Rice and N. G. Rice and R. Rieben and A. Rigatti and S. Riggs and H. G. Rinderknecht and K. Ring and B. Riordan and R. Riquier and C. Rivers and D. Roberts and V. Roberts and G.



https://doi.org/10.1017/hpl.2025.4 Published online by Cambridge University Press

Robertson and H. F. Robey and J. Robles and P. Rocha and G. Rochau and J. Rodriguez and S. Rodriguez and M. D. Rosen and M. Rosenberg and G. Ross and J. S. Ross and P. Ross and J. Rouse and D. Rovang and A. M. Rubenchik and M. S. Rubery and C. L. Ruiz and M. Rushford and B. Russ and J. R. Rygg and B. S. Ryujin and R. A. Sacks and R. F. Sacks and K. Saito and T. Salmon and J. D. Salmonson and J. Sanchez and S. Samuelson and M. Sanchez and C. Sangster and A. Saroyan and J. Sater and A. Satsangi and S. Sauers and R. Saunders and J. P. Sauppe and R. Sawicki and D. Sayre and M. Scanlan and K. Schaffers and G. T. Schappert and S. Schiaffino and D. J. Schlossberg and D. W. Schmidt and P. F. Schmit and J. M. Smidt and D. H. G. Schneider and M. B. Schneider and R. Schneider and M. Schoff and M. Schollmeier and C. R. Schroeder and S. E. Schrauth and H. A. Scott and I. Scott and J. M. Scott and R. H. H. Scott and C. R. Scullard and T. Sedillo and F. H. Seguin and W. Seka and J. Senecal and S. M. Sepke and L. Seppala and K. Sequoia and J. Severyn and J. M. Sevier and N. Sewell and S. Seznec and R. C. Shah and J. Shamlian and D. Shaughnessy and M. Shaw and R. Shaw and C. Shearer and R. Shelton and N. Shen and M. W. Sherlock and A. I. Shestakov and E. L. Shi and S. J. Shin and N. Shingleton and W. Shmayda and M. Shor and M. Shoup and C. Shuldberg and L. Siegel and F. J. Silva and A. N. Simakov and B. T. Sims and D. Sinars and P. Singh and H. Sio and K. Skulina and S. Skupsky and S. Slutz and M. Sluyter and V. A. Smalyuk and D. Smauley and R. M. Smeltser and C. Smith and I. Smith and J. Smith and L. Smith and R. Smith and R. Smith and M. Schölmerich and R. Sohn and S. Sommer and C. Sorce and M. Sorem and J. M. Soures and M. L. Spaeth and B. K. Spears and S. Speas and D. Speck and R. Speck and J. Spears and T. Spinka and P. T. Springer and M. Stadermann and B. Stahl and J. Stahoviak and J. Stanley and L. G. Stanton and R. Steele and W. Steele and D. Steinman and R. Stemke and R. Stephens and S. Sterbenz and P. Sterne and D. Stevens and J. Stevers and C. H. Still and C. Stoeckl and W. Stoeffl and J. S. Stolken and C. Stolz and E. Storm and G. Stone and S. Stoupin and E. Stout and I. Stowers and R. Strauser and H. Streckart and J. Streit and D. J. Strozzi and J. Stutz and L. Summers and T. Suratwala and G. Sutcliffe and L. J. Suter and S. B. Sutton and V. Svidzinski and G. Swadling and W. Sweet and A. Szoke and M. Tabak and M. Takagi and A. Tambazidis and V. Tang and M. Taranowski and L. A. Taylor and S. Telford and W. Theobald and M. Thi and A. Thomas and C. A. Thomas and I. Thomas and R. Thomas and I. J. Thompson and A. Thongstisubskul and C. B. Thorsness and G. Tietbohl and R. E. Tipton and M. Tobin and N. Tomlin and R. Tommasini and A. J. Toreja and J. Torres and R. P. J. Town and S. Townsend and J. Trenholme and A. Trivelpiece and C. Trosseille and H. Truax and D. Trummer and S. Trummer and T. Truong and D. Tubbs and E. R. Tubman and T. Tunnell and D. Turnbull and R. E. Turner and M. Ulitsky and R. Upadhye and J. L. Vaher and P. VanArsdall and D. VanBlarcom and M. Vandenboomgaerde and R. VanQuinlan and B. M. Van Wonterghem and W. S. Varnum and A. L. Velikovich and A. Vella and C. P. Verdon and B. Vermillion and S. Vernon and R. Vesey and J. Vickers and R. M. Vignes and M. Visosky and J. Vocke and P. L. Volegov and S. Vonhof and R. Von Rotz and H. X. Vu and M. Vu and D. Wall and J. Wall and R. Wallace and B. Wallin and D. Walmer and C. A. Walsh and C. F. Walters and C. Waltz and A. Wan and A. Wang and Y. Wang and J. S. Wark and B. E. Warner and J. Watson and R. G. Watt and P. Watts and J. Weaver and R. P. Weaver and S. Weaver and C. R. Weber and P. Weber and S. V. Weber and P. Wegner and B. Welday and L. Welser-Sherrill and K. Weiss and K. B. Wharton and G. F. Wheeler and W.

Whistler and R. K. White and H. D. Whitley and P. Whitman and M. E. Wickett and K. Widmann and C. Widmayer and J. Wiedwald and R. Wilcox and S. Wilcox and C. Wild and B. H. Wilde and C. H. Wilde and K. Wilhelmsen and M. D. Wilke and H. Wilkens and P. Wilkins and S. C. Wilks and E. A. Williams and G. J. Williams and W. Williams and W. H. Williams and D. C. Wilson and B. Wilson and E. Wilson and R. Wilson and S. Winters and P. J. Wisoff and M. Wittman and J. Wolfe and A. Wong and K. W. Wong and L. Wong and N. Wong and R. Wood and D. Woodhouse and J. Woodruff and D. T. Woods and S. Woods and B. N. Woodworth and E. Wooten and A. Wootton and K. Work and J. B. Workman and J. Wright and M. Wu and C. Wuest and F. J. Wysocki and H. Xu and M. Yamaguchi and B. Yang and S. T. Yang and J. Yatabe and C. B. Yeamans and B. C. Yee and S. A. Yi and L. Yin and B. Young and C. S. Young and C. V. Young and P. Young and K. Youngblood and J. Yu and R. Zacharias and G. Zagaris and N. Zaitseva and F. Zaka and F. Ze and B. Zeiger and M. Zika and G. B. Zimmerman and T. Zobrist and J. D. Zuegel and A. B. Zylstra, "Achievement of Target Gain Larger than Unity in an Inertial Fusion Experiment," Phys. Rev. Lett. 132, 065102 (2024). DOI: https://doi.org/10.1103/PhysRevLett.132.065102

4. R. Betti and O. A. Hurricane, "Inertial-confinement fusion with lasers," Nat. Phys. 12, 435-448 (2016). DOI: https://doi.org/10.1038/nphys3736
5. W. L. Kruer, *The physics of laser plasma interactions* (Addison-Wesley Publishing Co, United States, 1988).
6. R. E. Kidder, "Hot-electron preheat of laser-driven targets," Nucl. Fusion 21, 145-151 (1981). DOI:
7. D. Juraszek, "Introduction to Diagnostics Requirements for ICF," in *Advanced Diagnostics for Magnetic and Inertial Fusion*, P. E. Stott, A. Wootton, G. Gorini, E. Sindoni, and D. Batani, eds. (Springer US, Boston, MA, 2002), pp. 11-18.
8. P. M. Celliers, G. W. Collins, L. B. Da Silva, D. M. Gold, and R. Cauble, "Accurate measurement of laser-driven shock trajectories with velocity interferometry," Appl. Phys. Lett. 73, 1320-1322 (1998). DOI: https://doi.org/10.1063/1.121882
9. J. D. Kilkenny, W. W. Hsing, S. H. Batha, G. A. Rochau, T. C. Sangster, P. M. Bell, D. K. Bradley, H. Chen, J. A. Frenje, M. Gatu-Johnson, V. Y. Glebov, R. J. Leeper, A. J. Mackinnon, S. P. Regan, J. S. Ross, and J. l. Weaver, "National Diagnostic Working Group (NDWG) for inertial confinement fusion (ICF)/high-energy density (HED) science: The whole exceeds the sum of its parts," Rev. Sci. Instrum. 94(2023). DOI: https://doi.org/10.1063/5.0128650
10. K. W. Hill, M. Bitter, P. C. Efthimion, R. Ellis, L. Gao, M. B. Schneider, H. Chen, S. Ayers, M. A. Barrios, P. Beiersdorfer, P. M. Bell, R. Bettencourt, D. K. Bradley, D. Casey, M. J. Edwards, B. A. Hammel, M. C. Hermann, W. W. Hsing, O. S. Jones, R. L. Kauffman, O. L. Landen, D. A. Liedahl, T. Ma, A. G. MacPhee, J. D. Moody, R. C. Nora, P. Patel, H. A. Scott, V. A. Smalyuk, B. K. Spears, D. B. THorn, J. D. Kilkenny, S. P. Regan, D. Nelson, R. Jungquist, I. Shoup, M, Y. Maron, and M. S. del Rio, "Adapting High Resolution X-Ray Spectroscopy from MFE to Temperature and Density Measurements in ICF," in *26th IAEA Fusion Energy Conference*, 2016), Medium: ED; Size: PDF-file: 10 pages; size: 10.14 Mbytes.
11. P. M. Celliers and M. Millot, "Imaging velocity interferometer system for any reflector (VISAR) diagnostics for high energy density sciences," Rev. Sci. Instrum. 94(2023). DOI: https://doi.org/10.1063/5.0123439



https://doi.org/10.1017/hpl.2025.4 Published online by Cambridge University Press

12. R. M. Malone, B. C. Frogget, M. I. Kaufman, T. W. Tunnell, R. L. Guyton, I. P. Reinbachs, P. W. Watts, J. R. Celeste, P. M. Celliers, T. L. Lee, B. J. MacGowan, E. W. Ng, R. B. Robinson, and L. G. Seppala, "Overview of the line-imaging VISAR Diagnostic at the National Ignition Facility (NIF)," in *International Optical Design*, Technical Digest (CD) (Optica Publishing Group, 2006), ThA5.
13. A. M. Manuel, M. Millot, L. G. Seppala, G. Frieders, Z. Zeid, K. Christensen, and P. M. Celliers, "Upgrades to the VISAR-streaked optical pyrometer (SOP) system on NIF," in *SPIE Optical Engineering + Applications*, (SPIE, 2015), 959104.
14. Y. Yang, Y. Li, Z. Guan, C. Yang, S. Zhang, F. Wang, and T. Li, "A diagnostic system toward high-resolution measurement of wavefront profile," Opt. Commun. 456, 124554 (2020). DOI: https://doi.org/https://doi.org/10.1016/j.optcom.2019.124554
15. P. M. Celliers, D. J. Erskine, C. M. Sorce, D. G. Braun, O. L. Landen, and G. W. Collins, "A high-resolution two-dimensional imaging velocimeter," Rev. Sci. Instrum. 81(2010). DOI: https://doi.org/10.1063/1.3310076
16. R. F. Smith, J. H. Eggert, R. Jeanloz, T. S. Duffy, D. G. Braun, J. R. Patterson, R. E. Rudd, J. Biener, A. E. Lazicki, A. V. Hamza, J. Wang, T. Braun, L. X. Benedict, P. M. Celliers, and G. W. Collins, "Ramp compression of diamond to five terapascals," Nature 511, 330-333 (2014). DOI: https://doi.org/10.1038/nature13526
17. F. A. Maryum, H. Allen, R. F. Smith, A. Jay, S. L. Zachary, and W. S. David, "X-ray diffraction diagnostic design for the National Ignition Facility," in *SPIE Optical Engineering + Applications*, (SPIE, 2013), 88500N.
18. R. Malone, J. Bower, G. Capelle, J. Celeste, P. Celliers, B. Frogget, R. Guyton, M. Kaufman, G. Lare, T. Lee, B. MacGowan, S. Montelongo, E. Ng, Thomas, Jr., T. Tunnell, and P. Watts, "Fielding of an imaging VISAR diagnostic at the National Ignition Facility (NIF)," in *SPIE International Symposium Optical Science andTechnology 49th Annual Meeting*, (SPIE, 2004), 148-157.
19. B. Kozioziemski, B. Bachmann, A. Do, and R. Tommasini, "X-ray imaging methods for high-energy density physics applications," Rev. Sci. Instrum. 94(2023). DOI: https://doi.org/10.1063/5.0130689
20. L. A. Pickworth, B. A. Hammel, V. A. Smalyuk, H. F. Robey, R. Tommasini, L. R. Benedetti, L. Berzak Hopkins, D. K. Bradley, M. Dayton, S. Felker, J. E. Field, S. W. Haan, B. Haid, R. Hatarik, E. Hartouni, D. Holunga, M. Hoppe, Jr., N. Izumi, S. Johnson, S. Khan, T. Kohut, B. Lahmann, O. L. Landen, S. LePape, A. G. MacPhee, E. Marley, N. B. Meezan, J. Milovich, S. R. Nagel, A. Nikroo, A. E. Pak, R. Petrasso, B. A. Remington, N. G. Rice, H. A. Scott, P. T. Springer, M. Stadermann, C. Walters, K. Widmann, and W. W. Hsing, "Development of new platforms for hydrodynamic instability and asymmetry measurements in deceleration phase of indirectly driven implosions on NIF," Phys. Plasmas 25(2018). DOI: https://doi.org/10.1063/1.5039744
21. A. B. Zylstra, D. T. Casey, A. Kritcher, L. Pickworth, B. Bachmann, K. Baker, J. Biener, T. Braun, D. Clark, V. Geppert-Kleinrath, M. Hohenberger, C. Kong, S. Le Pape, A. Nikroo, N. Rice, M. Rubery, M. Stadermann, D. Strozzi, C. Thomas, P. Volegov, C. Weber, C. Wild, C. Wilde, D. A. Callahan, and O. A. Hurricane, "Hot-spot mix in large-scale HDC implosions at NIF," Phys. Plasmas 27(2020). DOI: https://doi.org/10.1063/5.0003779
22. X. Liang, X. Xie, J. Kang, Q. Yang, H. Wei, M. Sun, and J. Zhu, "Design and experimental demonstration of a high conversion efficiency OPCPA pre-amplifier for

petawatt laser facility," High Power Laser Science and Engineering 6(2018). DOI: https://doi.org/10.1017/hpl.2018.52

23. J. Zhu, X. Xie, M. Sun, J. Kang, Q. Yang, A. Guo, H. Zhu, P. Zhu, Q. Gao, X. Liang, Z. Cui, S. Yang, C. Zhang, and Z. Lin, "Analysis and construction status of SG-II 5PW laser facility," High Power Laser Science and Engineering 6(2018). DOI: https://doi.org/10.1017/hpl.2018.23
24. M. Sun, X. Xie, J. Zhu, X. Zhang, Y. Zhang, P. Zhu, A. Guo, J. Kang, H. Zhu, Q. Yang, and X. Liang, "Experimental demonstration of 1011 temporal contrast in pure nanosecond optical parametric chirped pulse amplifiers," Appl. Opt. 60, 2056-2061 (2021). DOI: https://doi.org/10.1364/AO.417726
25. P. Tzeferacos, M. Fatenejad, N. Flocke, C. Graziani, G. Gregori, D. Q. Lamb, D. Lee, J. Meinecke, A. Scopatz, and K. Weide, "FLASH MHD simulations of experiments that study shock-generated magnetic fields," High Energy Density Physics 17, 24-31 (2015). DOI: https://doi.org/https://doi.org/10.1016/j.hedp.2014.11.003
26. B. Fryxell, K. Olson, P. Ricker, F. X. Timmes, M. Zingale, D. Q. Lamb, P. MacNeice, R. Rosner, J. W. Truran, and H. Tufo, "FLASH: An Adaptive Mesh Hydrodynamics Code for Modeling Astrophysical Thermonuclear Flashes," The Astrophysical Journal Supplement Series 131, 273 (2000). DOI: https://doi.org/10.1086/317361